Noncommutative deformed cat states under decoherence

K. Berrada[1,2] and H. Eleuch[3,4]

[1]*Imam Mohammad Ibn Saud Islamic University (IMSIU), College of Science, Department of Physics, Riyadh 11623, Saudi Arabia*

[2]*The Abdus Salam International Centre for Theoretical Physics, Strada Costiera 11, Miramare-Trieste 34151, Italy*

[3]*Institute for Quantum Science and Engineering, Texas AM University, College Station, Texas 77843, USA*

[4]*Department of Applied Sciences and Mathematics, College of Arts and Sciences, Abu Dhabi University, Abu Dhabi 59911, UAE*

(Received 9 February 2019; published 29 July 2019)

This work has been motivated through the paper [42] by S. Dey on the nonclassical properties of the deformed harmonic oscillators. We study the dynamics of the nonclassical properties and nonlocal correlation for deformed coherent states superposition (DCSS) subjects to decoherence effect due to a dissipative interaction in deformed spaces. We consider two types of deformations, q deformation that describes a large class of deformed harmonic oscillators and L deformation that enters in the real possibilities of trapped ion systems. We find that such a kind of superposition, that gives rise to a richer phase space structure, the nonclassicality, squeezing, and entanglement can survive and they are robust against decoherence. The present results show that DCSS have less optical noise under dissipative dynamics in comparison with the usual Schrödinger cat states and may open new perspectives for the experimental observation of macro realism in quantum mechanics.

DOI: 10.1103/PhysRevD.100.016020

I. INTRODUCTION

In the last four decades, coherent states have been played a crucial role and offered a surprisingly rich structure in different branches of physics. These states have been firstly introduced by Schrödinger in order to give the connection between the quantum and classical formulations using quantum harmonic oscillator states [1]. These introduced states are described by Heisenberg Lie algebra whose generators are defined in terms of the annihilation and creation operators for the harmonic oscillator. Glauber employed these states to give a new description of the optical lights as an eigenstate of the annihilation operator $\hat{a}|\alpha\rangle = \alpha|\alpha\rangle$ [2]. Klauder developed a set of continuous states in which the basic theory of coherent states for arbitrary Lie groups was considered. These extensions provide several important physical applications. Later, the coherent states related to any Lie group (not only associated to the case of Heisenberg-Weyl group for harmonic oscillators) have been introduced by Perelomov [3,4] and Gilmore [5]. A particular case of these states are the spin coherent states related the SU(2) group and Peremelov and Barut-Girardello coherent states which are associated to the SU(1,1) group. These states describe a large set of quantum systems providing many applications in theoretical and mathematical physics [6–11].

Over last two decades, there have been several experimental demonstrations of nonclassical effect, such as photon antibunching [12], sub-Poissonian statistics [13], and squeezing [14]. Moreover, there exist interesting quantum effects, and related quantum states that are hard to prepare and to detect, namely superposition states exhibiting quantum interference effects [15]. Such states display the striking consequences of the superposition principle of quantum mechanics. Transient electronic states of this type have recently been prepared via pulsed excitation of atomic Rydberg wave packets [16]. Furthermore, superpositions of coherent states can be prepared in the motion of a trapped ion [17] with respect to the nonclassical effects, the coherent states turn out to define the limit between the classical and nonclassical behavior, so that they do not display any of these interesting features. In the squeezed light, we can squeeze the uncertainty region in one quadrature [18]. Several related studies have been conducted and used of the nature of nonclassical photons such as to enhance spectral resolution [19], quantum imaging [20], subwavelength measurement of atomic separation and discuss on antibunching [21], new coherent effects due to dipole-dipole interaction [22], and provide interesting effects on spatial propagation and quantum noise [23–27]. The nonclassical light is a popular field of research, and scientists are interested to discover more the underlying truth of quantum world.

Every natural object is in contact with its environment, so its dynamics is that of an open system; thus, the interaction between composite quantum systems and its

environment and understanding the dynamics for different physical quantities have attracted more interest. This interaction results in the system experiencing quantum noise which shows up in the system exhibiting fluctuations, decoherence, and possibly irreversible dissipative dynamics. On a fundamental level, time is basically physical quantity. So, the dynamical evolution is an important property of system, which makes the finite-time quantum interesting in the own right [28]. A well-known example is that in most of the models used to describe quantum open systems, the coherence of a state decays asymptotically to zero, where the entanglement dynamics exhibits entanglement sudden death in the decoherent environment [29]. The environment noise presented in the physical systems often determines the performance of quantum properties. Therefore, it is important to develop methods to estimate the level of noise in order to avoid the decay phenomenon under decoherence. Determining the environment parameters on a quantum system will be the main step to control its spoiling effects.

The feature of quantum mechanics which most distinguishes it from classical mechanics is the coherent superposition of distinct physical states. Many of the less intuitive aspects of quantum theory can be traced to this feature. The famous Schrödinger cat argument highlights problems of interpretation where macroscopic superposition states are allowed [30]. In fact, such states are widely used in new quantum technology and rapidly collapse to a classical mixture exhibiting interference features [31,32]. A key requirement of quantum information processing with DCSS is the generation of cat states in free propagating optical fields. This has been known to be extremely demanding using current technology because strong nonlinearity or precise photon counting measurements are required. Nonclassical effects are useful in quantum information theory. Squeezed states are highly nonclassical. However, sometimes they are difficult to generate, as there is no generalized setting available in the literature to construct them. Additional complications arise when one considers the underlying space-time structure to be noncommutative, where the space-time coordinates do not commute any more. The most commonly studied version of these space-time structures consists of replacing the standard set of commutation relations for the canonical coordinates x^μ by noncommutative versions, such as $[x^\mu, x^\nu] = i\hbar\theta^{\mu\nu}$, where $\theta^{\mu\nu}$ is taken to be a constant antisymmetric tensor. More interesting structures, leading for instance to minimal length and generalized versions of Heisenberg's uncertainty relations, are obtained when $\theta^{\mu\nu}$ is taken to be a function of the momenta and coordinates, e.g., [33–35]. Nonclassical states of the electromagnetic field and of the atomic center-of-mass motion have played an important role in recent year, due to their relation with fundamental problems in quantum mechanics and to the many possible applications, ranging from high-resolution spectroscopy to low noise communication of quantum computation. However, the generation of these states is usually a demanding experimental challenge. One of the most difficult tasks is the suppression of decoherence effects originating from the interaction of the quantum system under consideration with its environment [36]. More recently, much effort has been dedicated to the theoretical investigation of the entanglement and nonclassicality in noncommutative systems [37–41]. Here, we investigate the dynamics of the nonclassical properties and nonlocal correlation in deformed coherent states superposition (DCSS) within deformed spaces. We consider two types of deformation and explore the influence of the physical parameters on nonclassicality, squeezing, and entanglement in the presence of decoherence effect when the states are emerged initially in a vacuum environment. To the best of our knowledge, this paper is considered as the first one that includes and studies the effect of decoherence on theses topics. This study shows a new result and explains the time evolution of the entanglement and nonclassicality properties in deformed spaces under the dissipative environment. In comparison with the aforementioned papers, our present work from the phenomenological viewpoint might be more practical to explain some experimental observations of the dissipation on the nonclassical and entanglement in noncommutative systems subject to a realistic environment providing more hints for future investigation on this topic.

The paper is organized as follows. In Sec. II, we give the main properties of the deformed-states superposition. The definition of the deformed commutator relation and the coherent states associated with the deformed boson operators in q- and L-deformed space for two kinds of deformations are summarized. In Sec. III, we study the nonclassicality and entanglement in the DCSS under decoherence effect due to a dissipative interaction. A summary and some conclusions are given in Sec. IV.

II. DEFORMED-STATES SUPERPOSITION

Several advantages of utilizing DCSS over the undeformed case, like the enhancement of the squeezing of the quadrature beyond the nondeformed case and improvement of various tasks in quantum optics and information. We choose to study the time variation of the classical properties for Schrödinger cat states in a deformed space under decoherence effect using numerous quantum quantifiers. The interferometric setup generally consists of different steps. The first is the preparation step where the input state is chosen as a coherent superposition states, $\rho_{\rm int}$. In this context, we will demonstrate that moderate size of DCSS offers advantage in comparison with usual Schrödinger cat state. This needs to consider how such states could be implemented in order to realize this advantage. After the preparation step, the output mixed state $\rho_{\rm out}$ is subjected to

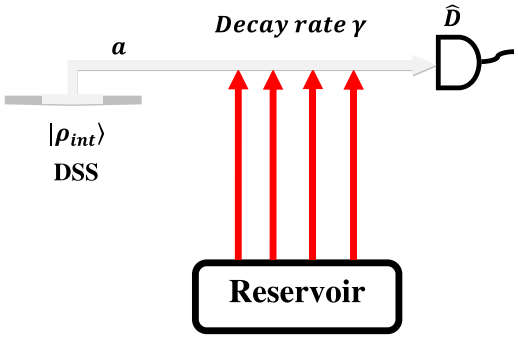

FIG. 1. It shows an interferometric setup for the DCSS. The input state is fed into an interferometer through one channel which is subjected to a dissipative effect during the evolution.

dissipation effect. Finally, the output state is measured for the nonclassical properties and entanglement (see Fig. 1).

The aim of this manuscript is to describe the behavior of the nonclassical properties for a nonlinear oscillator described through Schorödinger cat states in deformed spaces, like the f oscillator, plunged in a bath modeled by an assembly of harmonic oscillators. We choose here a f-deformed algebra which has been shown to be related to the noncommutative space-time structures leading to the existence of minimal lengths and minimal momenta as a result of generalized uncertainty relation [42]. We identify several advantages of utilizing these kind of deformed spaces rather than the usual quantum mechanical systems. The Hamiltonian of an f-deformed oscillator may be taken, in the case of unitary frequency and natural units, as

$$H = \frac{\hbar}{2}(A^\dagger A + AA^\dagger), \tag{1}$$

where the operators A and $A^\dagger$ result as a distortion of the usual annihilation and creation operators a and $a^\dagger$. The operators A and $A^\dagger$ therefore obey the following nonlinear commutator algebras [43]:

$$[A, n] = A, \qquad [A^\dagger, n] = -A^\dagger, \tag{2}$$

as for the usual nondeformed boson operators. Note that in this definition one does not require A and $A^\dagger$ to be related to n in the usual way, i.e., in general $A^\dagger A \neq n$. The vacuum state $|0\rangle$ does not contain quanta, therefore $n|0\rangle = 0$ and $A|0\rangle = 0$. The product $A^\dagger A$ preserves the number of quanta; consequently, it is necessarily a function of n. A convenient notation of a box function is introduced $A^\dagger A = [n]$ (read "box n). Similarly, $AA^\dagger$ is also a function of n and it can be shown that $AA^\dagger = [n+1]$. The deformed commutation relation is defined by

$$AA^\dagger - A^\dagger A = [n+1] - [n]. \tag{3}$$

The q-deformed oscillators may be considered as special cases of the so-called f oscillators, where the f-oscillator operators have been defined by

$$A = af(n) = f(n+1)a,$$
$$A^\dagger = f(n)a^\dagger = a^\dagger f(n+1), \tag{4}$$

and

$$[A, A^\dagger] = (n+1)f^2(n+1) - nf^2(n), \tag{5}$$

where $f(n)$ is an operator-valued function of the Hermitian number operator $n = a^\dagger a$. The nonlinearity arises from $f(n)$. The function f, which is a characteristic for the deformation, has a dependence on a deformation parameter q such that when the deformation disappears, then $f(n) = 1$. The deformed algebra reduces to the Heisenberg algebra

$$[a, a^\dagger] = 1, \qquad [n, a] = -a \quad \text{and} \quad [n, a^\dagger] = a^\dagger. \tag{6}$$

Transformation (4) of the operators $a, a^\dagger$ to $A, A^\dagger$ represents a nonlinear noncanonical transformation, since it does not preserve the commutation relation, i.e., $[A, A^\dagger] \neq 1$. The operators $A^\dagger$ and A act as raising and lowering in the noncommutative space

$$A^\dagger|n\rangle = \sqrt{[n+1]_f}|n+1\rangle,$$
$$A|n\rangle = \sqrt{[n]_f}|n-1\rangle. \tag{7}$$

The states $|n\rangle$ form an orthonormal basis in deformed Hilbert space spanned by the vectors $|\psi\rangle = \sum_{n=0}^{\infty} c_n|n\rangle$ with $c_n \in \mathcal{C}$ such that $\langle\psi|\psi\rangle = \sum_{n=0}^{\infty}|c_n|^2 < \infty$.

In analogy to the Glauber states, the f-coherent states are therefore defined as the right eigenvector of the f-deformed bosonic field A,

$$A|\xi, f\rangle = \xi|\xi, f\rangle, \tag{8}$$

where ξ is a complex eigenvalue, which is however allowed as A is non-Hermitian. In general, it can be made dependent on continuous parameters, in such a way that, for given particular values, the usual algebra is recovered. The f-coherent state can be written as

$$|\xi, f\rangle = \mathcal{N}_f \sum_{n=0}^{\infty} \frac{\xi^n}{\sqrt{[n]_f!}}|n\rangle, \qquad \mathcal{N}_f = [\exp_f[|\xi|^2]]^{-\frac{1}{2}}, \tag{9}$$

and we have introduced

$$\exp_f[x] = \sum_{n=0}^{\infty} \frac{x^n}{[n]_f!},$$
$$[n]_f! = [nf^2(n)] \times [(n-1)f^2(n-1)] \times \cdots \times [f(1)]. \quad (10)$$

The function $\exp_f$ is a deformed version of the usual exponential function. They become coincident when f is the identity. Notice that $\exp_f[x]\exp_f[y] \neq \exp_f[x+y]$, i.e., we have a nonextensive exponential which can be found in many physical problems. Then, let us consider two types of deformations. The q deformation defined by [44]

$$f(n) = \left[\frac{1}{n}\frac{1-q^{-n}}{q-1}\right]^{-\frac{1}{2}}, \qquad q \in \mathbb{R}, \quad (11)$$

and the deformation given by [45]

$$f(n) = \frac{L_n^1(\eta^2)}{(n+1)L_n^0(\eta^2)}, \qquad \eta \in \mathbb{R}, \quad (12)$$

which we are going to name L deformation, since L_n^m indicates the associate Laguerre polynomial. It is worth noting that such L deformation naturally arises in ion-trapped systems [45]. These states emerge as stationary states of the motion of an appropriately laser-driven trapped ion, which is in the resolved sideband limit and far from the Lamb-Dicke regime [45]. Clearly, $f(n) = 1$ when $\eta = 0$ and in this case nonlinear coherent states become the standard coherent states. However, when $\eta \neq 0$, nonlinearity starts developing with the degree of nonlinearity depending on the magnitude of η.

We focus on the nonclassical properties and entanglement for two kinds of deformations and different strength regimes of the DCSS under dissipative Markovian dynamics. In Fig. 1, the input state is chosen to be

$$|\Psi\rangle = \mathcal{N}_+(|\xi, f\rangle + |-\xi, f\rangle),$$
$$\mathcal{N}_+ = [2 + 2\mathcal{N}_f^2 \exp_f[-|\xi|^2]]^{-\frac{1}{2}}. \quad (13)$$

The search for physically inspired Hamiltonians, which may display definite features about q-deformation effects, is still open. Concrete applications of the formalism have been explored more recently [46–49] and these complement previous mathematical efforts, such as studies of generalized q-deformed oscillators [50,51]. Moreover, it is shown that the q deformation plays a significant role in understanding higher-order effects in the many-body interaction [52]. Then, the notion of deformed coherent states was straightforwardly introduced, and the generation of such nonlinear coherent states enters in the real possibilities of trapped systems. Microlasers (and especially single-atom lasers) are known to be sources of nonclassical light. It has already been shown that a single-atom laser, considered within the scope of the strong-coupling regime, can produce special kind of nonlinear coherent states, namely, Mittag-Leffler coherent states [53].

In the following, we shall determine the dynamical behavior of the DCSS in the realistic scenario of the photon loss. In other words, we wish to see how the DCSS resists to photon loss in comparison with the usual Schrödinger cat states for different values of physical parameters in the presence of loss. To this end, we introduce the decoherence effects due to a dissipative interaction with the environment. This can be described by the following master equation of the Lindblad form:

$$\dot{\rho}_{\text{out}} = \gamma a \rho_{\text{out}} a^\dagger - \frac{\gamma}{2}\{a^\dagger a, \rho\}, \quad (14)$$

where γ is the damping rate, and we have set the bath temperature equal to zero. The decoherence effect on the state $\rho_{\text{out}}(0) = |\Psi_{\text{out}}\rangle\langle\Psi_{\text{out}}|$ can be described in the following way [54]:

$$\rho_{\text{out}}(t) = \sum_{k=0}^{\infty} \Gamma_k(t)\rho_{\text{out}}(0)\Gamma_k^\dagger(t), \quad (15)$$

where

$$\Gamma_k(t) = \sum_{n=k}^{\infty} \binom{n}{k}^{\frac{1}{2}} [\eta(t)]^{(n-k)/2}[1-\eta(t)]^{k/2}|n-k\rangle\langle n|, \quad (16)$$

with $\eta(t) = e^{-\gamma t}$. Here, we are not interested in the dynamics in the presence of a deformed Hamiltonian [54]. Using the truncated density matrix $\rho_{\text{out}}(t)$ for different input states, we obtain numerically the nonclassical properties and nonlocal correlation under decoherence effect. The results show that DCSS, for both q-deformed and L-deformed cases, clearly preserves the loss of nonclassical and correlation properties achieved by undeformed sates under decoherence effect, for a wide range of the dimensionless time. This effect wins out the fact that, by a proper choice of the physical parameters, the photon losses due to dissipative do not destroy the coherence in their superposition and maintain their nonclassical properties.

III. PHYSICAL PROPERTIES OF DEFORMED CAT STATES

In this section, we will calculate the photon distribution function, Mandel's parameter, and quadrature dispersion in the introduced deformed-states superposition under decoherence. It is possible to calculate these quantities explicitly [55,56]. Since

$$a = \sum_{n=0}^{\infty} \sqrt{n}\,|n-1\rangle\langle n|, \quad (17)$$

$$a^\dagger = \sum_{n=0}^{\infty} \sqrt{n}\,|n\rangle\langle n-1|, \quad (18)$$

the same Fock space is a carrier space for A and $A^\dagger$, i.e.,

$$A = \sum_{n=0}^{\infty} \sqrt{n}\, f(n)|n-1\rangle\langle n|, \tag{19}$$

$$A^{\dagger} = \sum_{n=0}^{\infty} \sqrt{n}\, f^{*}(n)|n\rangle\langle n-1|. \tag{20}$$

We will take advantage of equations, which gives the expression

$$a = \frac{1}{f(n+1)} A,$$

and

$$a^{\dagger} = A^{\dagger} \frac{1}{f(n+1)}. \tag{21}$$

A. Photon number function

To obtain the photon distribution function, we have to calculate the probability P_n to have n photons in the deformed cat state with the density operator $\hat{\rho}$. This probability is given by

$$P_n(t) = \mathrm{Tr}[\hat{\rho}(t)|n\rangle\langle n|]. \tag{22}$$

The function P_n may be obtained in we calculate the generating function for the matrix element $\hat{\rho}_{mn}(t)$ of the density operator $\hat{\rho}(t)$ in the Fock basis. For usual harmonic oscillators, this generating function is the matrix element of the density operator in the coherent state basis

$$\langle\beta|\hat{\rho}(t)|\alpha\rangle = \exp\left(-\frac{|\alpha|^2}{2} - \frac{|\beta|^2}{2}\right) \sum_{m,n=0}^{\infty} \frac{\bar{\beta}^m \alpha^n}{\sqrt{m!n!}} \rho_{mn}, \tag{23}$$

and

$$P_n(t) = \rho_{nn}(t). \tag{24}$$

The function $\langle\alpha|\hat{\rho}(t)|\alpha\rangle$ is the Q function of the system with the density operator $\hat{\rho}(t)$. The coherent state $|\alpha\rangle$ is the normalized eigenstate of the annihilation operator

$$a|\alpha\rangle = \alpha|\alpha\rangle. \tag{25}$$

Using Eq. (15), we obtain for the photon distribution function P_n

$$P_n(t) = (\mathcal{N}_f \mathcal{N}_+)^2 \sum_{k=0}^{\infty} \frac{(n+k)!}{n!k!} [\eta(t)]^n [1-\eta(t)]^k \times \left[\frac{(1+(-1)^{n+k})^2}{[n+k]_f!} |\xi|^{2n+2k}\right]. \tag{26}$$

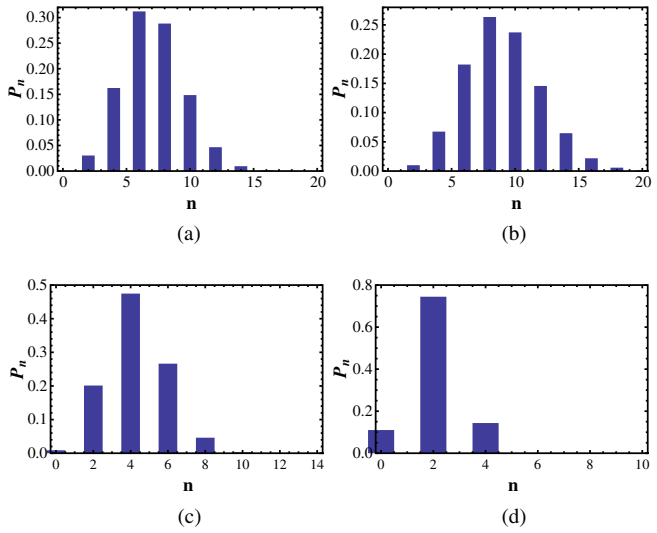

FIG. 2. Photon distribution function of the DCSS as a function of the number of photon for q deformation in the absence of decoherence effect ($t = 0$). (a) is for $q = 0.95$ and $|\xi| = 3$, (b) is for $q = 1$ and $|\xi| = 3$, (c) is for $q = 0.8$ and $|\xi| = 3$, and (d) is for $q = 0.5$ and $|\xi| = 3$.

The expression (26) is a partial case of the matrix elements of the density operator in Fock states basis.

In Figs. 2 and 3, we display the photon distribution function in the absence of decoherence effect by choosing different values of the q deformation and L deformation, respectively. From the figures, we can observe that the probability of finding odd and even photons in DCSS is strictly dependent on the value and kind of the deformation in the deformed space, which provides a strong evidence of

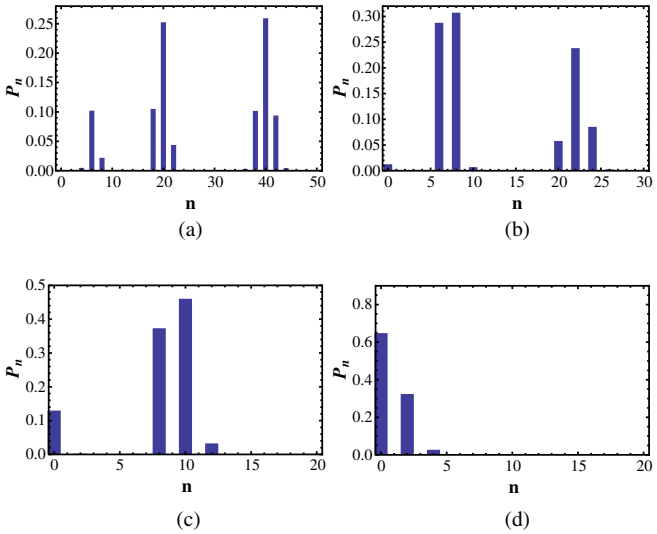

FIG. 3. Photon distribution function of the DCSS as a function of the number of photon for L deformation in the absence of decoherence effect ($t = 0$). (a) is for $\eta = 0.85$ and $|\xi| = 1$, (b) is for $\eta = 0.8$ and $|\xi| = 1$, (c) is for $\eta = 0.7$ and $|\xi| = 1$, and (d) is for $\eta = 0$ and $|\xi| = 1$.

nonclassicality. In Fig. 4, we plot the photon distribution function as a function of the dimensionless time γt for various values of the different physical parameters. We immediately see that the probability decreases with increasing time and it reaches a minimum value as the time becomes significantly large. Interestingly, we find that the amount of the probability for the different kinds of deformations is shown to be large than the usual case ($q = 1$ and $\eta = 0$). Furthermore, the larger the value of $|\xi|$ is, the larger the value of the critical time for which the probability is minimal.

B. Photon counting statistics

We now investigate the influence of decoherence effect on the sub-Poissonian statistics of the radiation field. For this purpose, we calculate the Mandel's parameter defined by

$$Q(t) = \frac{(\langle n(t)^2\rangle - \langle n(t)\rangle^2)}{\langle n(t)\rangle} - 1. \tag{27}$$

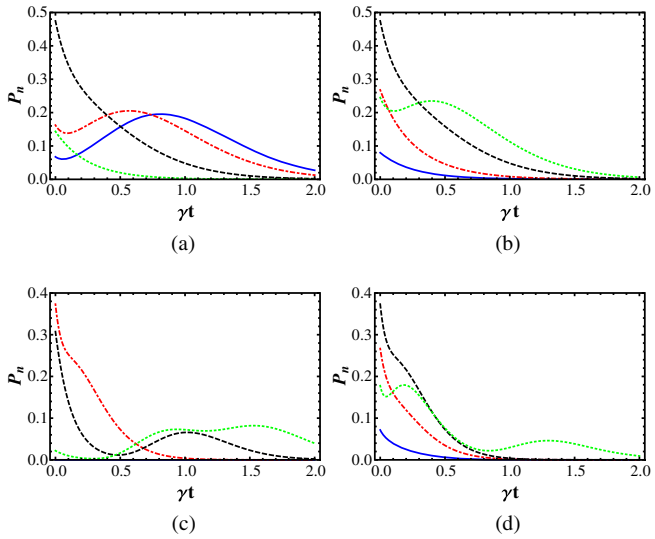

FIG. 4. Photon distribution function as a function of dimensionless time γt for various values of the deformed parameter and amplitude for both q deformation and L deformation. (a) The time evolution of the photon distribution function for various values of the parameter q with $|\xi| = 3$ and $n = 4$. The blue line is for $q = 1$, red line is for $q = 0.95$, black line is for $q = 0.8$, and green line is for $q = 0.5$. (b) The time evolution of the photon distribution function for various values of $|\xi|$ with $q = 0.8$ and $n = 4$. The blue line is for $|\xi| = 1.5$, red line is for $|\xi| = 2$, black line is for $|\xi| = 3$, and green line is for $|\xi| = 4$. (c) The time evolution of the photon distribution function for various values of the parameter η with $|\xi| = 1$ and $n = 8$. The blue line is for $\eta = 0$, red line is for $\eta = 0.7$, black line is for $\eta = 0.8$, and green line is for $\eta = 0.85$. (d) The time evolution of the photon distribution function for various values of $|\xi|$ with $\eta = 0.7$ and $n = 8$. The blue line is for $|\xi| = 0.8$, red line is for $|\xi| = 0.9$, black line is for $|\xi| = 1$, and green line is for $|\xi| = 1.2$.

For $Q < 0$ ($Q > 0$), the statistics is sub-Poissonian (super-Poissonian); $Q = 0$ stands for Poissonian statistics. Since $\langle n(t)\rangle = \sum_{n=0}^{\infty} nP_n(t)$ and $\langle n(t)^2\rangle = \sum_{n=0}^{\infty} n^2P_n(t)$, we have

$$Q(t) = \frac{(\sum_{n=0}^{\infty} n^2P_n(t)) - (\sum_{n=0}^{\infty} nP_n(t))^2}{\sum_{n=0}^{\infty} nP_n(t)} - 1, \tag{28}$$

where the probability of finding n photons in the radiation field is given by Eq. (26).

Figure 5 shows the parameter $Q(t)$ as a function of the dimensionless time γt for various values of the deformed parameters (q and η) and the amplitude ξ. It is worth noting that a remarkable behavior of the parameter $Q(t)$ under decoherence is strictly related to initial nature of the photon distribution in the DCSS. When $Q > 0$ at $t = 0$, the parameter $Q(t)$ decreases monotonically with increasing γt and approaches zero ($Q \simeq 0$ for large values of times). So we therefore find that the decoherence leads to decrease the degree of the nonclassicality in the DCSS. When $Q < 0$ at $t = 0$, the Mandel's parameter increases with increasing time γt and vanishes as the time becomes significantly

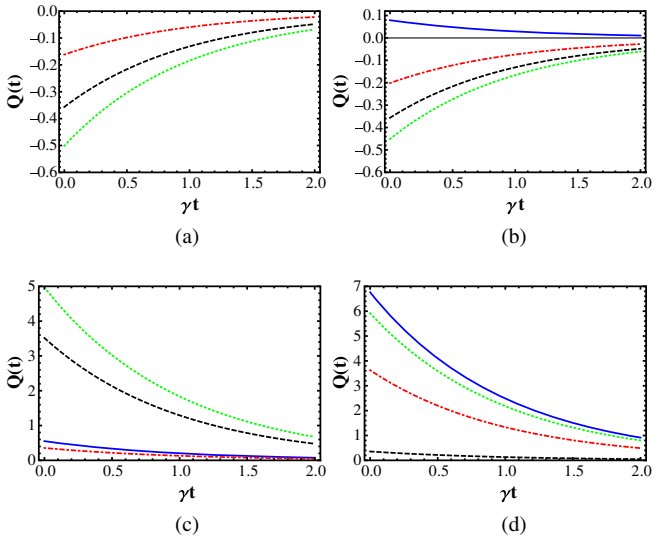

FIG. 5. Mandel's parameter as a function of dimensionless time γt for various values of the deformed parameter and amplitude for both q deformation and L deformation. (a) The time evolution of the Mandel's parameter for various values of the parameter q with $|\xi| = 3$. The blue line is for $q = 1$, red line is for $q = 0.95$, black line is for $q = 0.8$, and green line is for $q = 0.5$. (b) The time evolution of the Mandel's parameter for various values of $|\xi|$ with $q = 0.8$. The blue line is for $|\xi| = 1.5$, red line is for $\xi = 2$, black line is for $|\xi| = 3$, and green line is for $|\xi| = 4$. (c) The time evolution of the Mandel's parameter for various values of the parameter η with $|\xi| = 1$. The blue line is for $\eta = 0$, red line is for $\eta = 0.7$, black line is for $\eta = 0.8$, and green line is for $\eta = 0.85$. (d) The time evolution of the Mandel's parameter for various values of $|\xi|$ with $\eta = 0.7$. The blue line is for $|\xi| = 0.8$, red line is for $|\xi| = 0.9$, black line is for $|\xi| = 1$, and green line is for $|\xi| = 1.2$.

large. The nonclassicality is determined by the values of deformed parameter and the amplitude. If one considers the q-deformed case, the photon distribution remains sub-Poissonian where the states are highly nonclassical for larger value of $|\xi|$ and as q gets farther from the undeformed case, the Mandel's parameter becomes more and more negative, which does not happen for the usual Schrödinger cat states. While in the case of L deformation, the physical parameters act differently exhibiting super-Poissonian distribution. From these results, we find that the preservation and enhancement of the nonclassicality in the deformed space under decoherence effect can benefit from the combination of the deformed parameter and the amplitude. In other words, the impact of the decoherence on the photon distribution of DCSS depends on the kind of deformation in the deformed space. It is worth to mention here that we have examined the Mandel's parameter for a wide range of deformed parameter and amplitude and obtained the same qualitative behavior.

C. Quadrature squeezing

Here we study the dynamical behavior of the quadrature squeezing of the DCSS. In order to do so, let us consider the following hermitian quadrature operators [42,57]:

$$X_1 = \frac{A + A^\dagger}{2}, \qquad Y_1 = \frac{A - A^\dagger}{2i}. \tag{29}$$

The operators X_1 and Y_1 satisfy the following uncertainty relation:

$$\langle \Delta X_1^2 \rangle \langle \Delta Y_1^2 \rangle \geq \frac{1}{16}, \tag{30}$$

where the variance of X_1 is defined as $\langle \Delta X_1^2 \rangle = \langle X_1^2 \rangle - \langle X_1 \rangle^2$. A state of the radiation field is squeezed when

$$\langle \Delta X_1^2 \rangle < \frac{1}{4}, \tag{31}$$

or

$$\langle \Delta Y_1^2 \rangle < \frac{1}{4}, \tag{32}$$

which can be expressed in terms of the annihilation and creation operators, A and $A^\dagger$. The expectation values of X_1 and X_1^2 are determined by

$$\begin{aligned}\langle X_1 \rangle &= \frac{1}{2}\mathrm{Tr}[\rho(t)(A + A^\dagger)] \\ &= \frac{1}{2}\left[\sum_n \sqrt{[n+1]_f}\,\rho_{n+1,n}(t) + \sum_n \sqrt{[n]_f}\,\rho_{n-1,n}(t)\right],\end{aligned}$$

and

$$\begin{aligned}\langle X_1^2 \rangle &= \frac{1}{4}\mathrm{Tr}[\rho(t)(A^2 + AA^\dagger + A^\dagger A + (A^\dagger)^2)] \\ &= \frac{1}{4}\left[\sum_n \sqrt{[n+1]_f[n+2]_f}\,\rho_{n+2,n}(t) + \sum_n [n]_f \rho_{n,n}(t)\right. \\ &\quad \left. + \sum_n [n+1]_f \rho_{n,n}(t) + \sum_n \sqrt{[n]_f[n-1]_f}\,\rho_{n-2,n}(t)\right],\end{aligned}$$

and similarly for the other quadrature Y_1, we have

$$\begin{aligned}\langle Y_1 \rangle &= \frac{1}{2i}\mathrm{Tr}[\rho(t)(A - A^\dagger)] \\ &= \frac{1}{2i}\left[\sum_n \sqrt{[n+1]_f}\,\rho_{n+1,n}(t) - \sum_n \sqrt{[n]_f}\,\rho_{n-1,n}(t)\right],\end{aligned}$$

and

$$\begin{aligned}\langle Y_1^2 \rangle &= -\frac{1}{4}\mathrm{Tr}[\rho(t)(A^2 - AA^\dagger - A^\dagger A + (A^\dagger)^2)] \\ &= -\frac{1}{4}\left[\sum_n \sqrt{[n+1]_f[n+2]_f}\,\rho_{n+2,n}(t) - \sum_n [n]_f \rho_{n,n}(t)\right. \\ &\quad \left. - \sum_n [n+1]_f \rho_{n,n}(t) + \sum_n \sqrt{[n]_f[n-1]_f}\,\rho_{n-2,n}(t)\right],\end{aligned}$$

where

$$\begin{aligned}\rho_{m,n}(t) = (\mathcal{N}_+\mathcal{N}_f)^2 \sum_{k=0}^{\infty} &\left[\binom{m+k}{k}\binom{n+k}{k}\right]^{\frac{1}{2}} [\eta(t)]^{\frac{m}{2}} \\ &\times [\eta(t)]^{\frac{n}{2}}[1-\eta(t)]^k \left[\frac{\xi^{(m+k)} + (-\xi)^{(m+k)}}{\sqrt{[m+k]_f!}}\right] \\ &\times \left[\frac{\bar{\xi}^{(n+k)} + (-\bar{\xi})^{(n+k)}}{\sqrt{[n+k]_f!}}\right].\end{aligned}$$

We now evaluate the inequalities in Eqs. (31) and (32), and the results are represented in Fig. 6. In Fig. 6, we have displayed the graphs of $\langle \Delta X_1^2 \rangle$ and $\langle \Delta Y_1^2 \rangle$ as a function of the time γt for the two kinds of deformations with different values of the physical parameters. We observe that while the curve of $\langle \Delta X_1^2 \rangle$ is greater than $1/4$ that of $\langle \Delta Y_1^2 \rangle$ is less than $1/4$ for a wide range of γt. Thus, by a proper choice of the physical parameters, one of the inequalities in (31) and (32) is satisfied. This implies that the quadrature squeezing of DCSS may result much more robust against decoherence than their undeformed version for a wide range of the time interval.

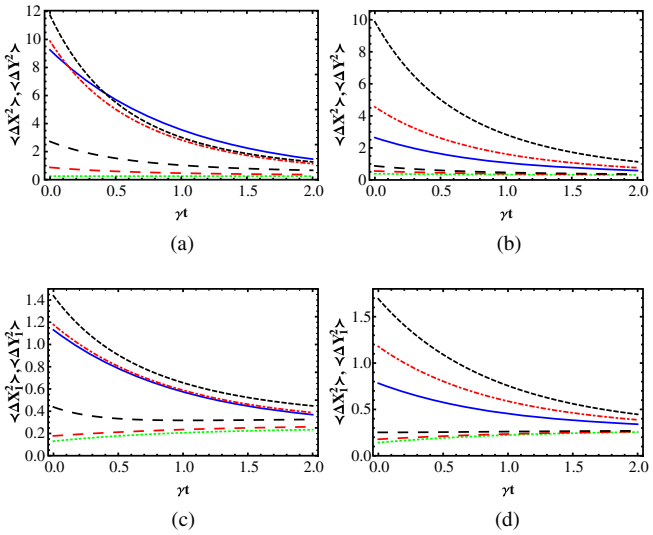

FIG. 6. Quadrature squeezing as a function of dimensionless time γt for various values of the deformed parameter and amplitude for both q deformation and L deformation. (a) The time evolution of the quadrature squeezing for various values of the parameter q with $|\xi| = 3$. The blue line is for $\langle \Delta X_1^2 \rangle$ with $q = 1$, dash-dotted red line is for $\langle \Delta X_1^2 \rangle$ with $q = 0.8$, dashed black line is for $\langle \Delta X_1^2 \rangle$ with $q = 0.5$, dotted green line is for $\langle \Delta Y_1^2 \rangle$ with $q = 1$, red long dashed line is for $\langle \Delta Y_1^2 \rangle$ with $q = 0.8$, and black long dashed line is for $\langle \Delta Y_1^2 \rangle$ with $q = 0.5$. (b) The time evolution of the quadrature squeezing for various values of $|\xi|$ with $q = 0.8$. The blue line is for $\langle \Delta X_1^2 \rangle$ with $|\xi| = 1.5$, dash-dotted red line is for $\langle \Delta X_1^2 \rangle$ with $|\xi| = 2$, dashed black line is for $\langle \Delta X_1^2 \rangle$ with $|\xi| = 3$, dotted green line is for $\langle \Delta Y_1^2 \rangle$ with $|\xi| = 1.5$, red long dashed line is for $\langle \Delta Y_1^2 \rangle$ with $|\xi| = 2$, and black long dashed line is for $\langle \Delta Y_1^2 \rangle$ with $|\xi| = 3$. (c) The time evolution of the quadrature squeezing for various values of the parameter η with $|\xi| = 1$. The blue line is for $\langle \Delta X_1^2 \rangle$ with $\eta = 0$, dash-dotted red line is for $\langle \Delta X_1^2 \rangle$ with $\eta = 0.3$, dashed black line is for $\langle \Delta X_1^2 \rangle$ with $\eta = 0.5$, dotted green line is for $\langle \Delta Y_1^2 \rangle$ with $\eta = 0$, red long dashed line is for $\langle \Delta Y_1^2 \rangle$ with $\eta = 0.3$, and black long dashed line is for $\langle \Delta Y_1^2 \rangle$ with $\eta = 0.5$. (d) The time evolution of the quadrature squeezing for various values of $|\xi|$ with $\eta = 0.3$. The blue line is for $\langle \Delta X_1^2 \rangle$ with $|\xi| = 0.8$, dash-dotted red line is for $\langle \Delta X_1^2 \rangle$ with $|\xi| = 1$, dashed black line is for $\langle \Delta X_1^2 \rangle$ with $|\xi| = 1.2$, dotted green line is for $\langle \Delta Y_1^2 \rangle$ with $|\xi| = 0.8$, red long dashed line is for $\langle \Delta Y_1^2 \rangle$ with $\xi = 1$, and black long dashed line is for $\langle \Delta Y_1^2 \rangle$ with $|\xi| = 1.2$.

D. Quantum entanglement

Due to the promise of quantum computation, there is currently considerable interest in the relationship between entanglement, decoherence, entropy, and measurement. Motivated by quantum information theory several authors have recently investigated entanglement in quantum many-body systems [58–60]. It is often stated that decoherence or a measurement causes a system to become entangled with its environment. The purpose of this paper is to make these ideas quantitative by a study of the model, the DCSS model. This describes a DCSS interacting with an infinite collection of harmonic oscillators that model the environments responsible for decoherence and dissipation. Specifically, we show how the entanglement between a superposition state of the deformed states and the environment changed in terms of the physical parameters. One interesting result is that we find that the DCSS becomes maximally entangled with the environment depending on the values of the amplitude and deformed parameter. The entanglement of the DCSS-environment state under dissipative Markovian dynamics can be quantified in terms of the von Neumann entropy since the whole state is pure, which is generally defined for a bipartite state ρ_{SE} as

$$S(t) = -\mathrm{Tr}(\rho_S(t) \ln \rho_S(t)) = -\sum_i r_i(t) \ln r_i(t), \quad (33)$$

where $\rho_S(t) = \mathrm{Tr}_E(\rho_{SE}(t))$ is the reduced density matrix of DCSS, and $r_i(t)$ is its eigenvalues.

In Fig. 7, the von Neumann entropy is displayed as a function of the dimensionless time for various values of deformation parameter and amplitude. Solid line is for $|\xi| = 1$ and dashed line is for $|\xi| = 3$. We observe that the von Neuman entropy exhibits a sudden rise to the maximal value, indicating that the dissipative interaction effect may enhance the correlation between the DCSS and its environment in this range of time, and suppressed to the zero value as the time becomes significantly large. We also find that the degree of entanglement for the q deformation and L deformation is shown to be large than the undeformed case. Furthermore, the increase in the value of the amplitude ξ may retard the entanglement loss between the DCSS and its environment during the time evolution. The vanishing phenomenon of the entanglement with time reflects that the DCSS-environment state becomes unentangled, which can understood as following: in the Markovian dynamics, the correlations between the open system and

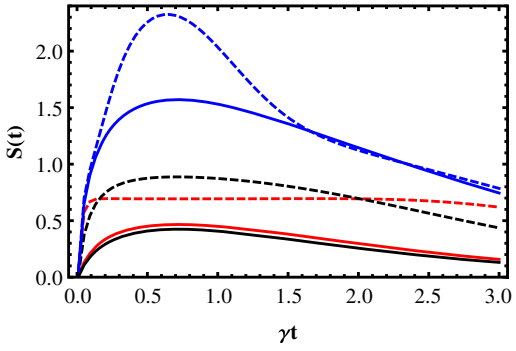

FIG. 7. The von Neumann entropy for the DCSS field under dissipative effect [54] is plotted as a function of time γt for various values of the amplitude $|\xi|$. Solid line is for $|\xi| = 1$ and dashed line is for $|\xi| = 3$. The red curve is for undeformed case ($q = 1$ or $\eta = 0$), black curve is for q deformation ($q = 0.5$), and blue curve is for L deformation ($\eta = 0.7$).

its environment as well as the changes in the environmental state due to the interaction do not have a significant influence on the subsequent evolution of the open system as the time tends to infinity. This picture is often introduced relying on qualitative considerations, possibly assuming that the total state at time can be effectively represented as a product state between the state of the open system and a fixed state of the environment. For long times, losses finally transfers all photons from the system to the environment, leaving with a pure of the system vacuum which of course is not entangled state.

IV. CONCLUSION

We have studied the time evolution of several like nonclassical properties and entanglement in DCSS subjects to dissipative interaction in q- and L-deformed space. We have explored several advantages of utilizing this kind of noncommutative space for cat states rather than the usual quantum mechanical systems under decoherence effect. We have shown that such kind of superposition, the nonclassicality and entanglement phenomena can be more robust against decoherence than the usual Schrödinger cat states. These states, due to their nonlinear character, give rise to a richer phase space structure, part of which can more easily survive against decoherence. In particular, we have found that by a proper choice of the deformed parameter and the amplitude of cat states in noncommutative space leads to preserve the squeezing of the quadrature, sub-Poissonian and super-Poissonian distribution, and nonlocal correlation beyond the ordinary case under decoherence effect. Interestingly, the degree of those properties for q deformation and L deformation is shown to be interesting in comparison with usual case as the amplitude becomes significantly large. The present results may open new preservatives for the experimental observation of macroscopic realism in quantum mechanics in the framework of deformed algebra which has been shown to be related to the noncommutative space-time structures, leading to the existence of minimal lengths and minimal momenta as a result of generalized uncertainty relation. These results may be experimentally realized and contribute to new advance technology to produce DCSS, which may open new perspectives for future research avenues. In comparison with some recent work on the dissipation of the DCSS system, our present work from the phenomenological viewpoint might be more practical to explain some experimental observations of the dissipation on the nonclassicality and entanglement subject to a realistic environment providing more hints for future investigation on this topic. We note that we treat here the time evolution of nonclassical properties and nonlocal correlation under the effect of zero-temperature reservoir. Certainly, a study of how the thermal bath affects these properties will make a useful contribution to more understanding the dynamics of these properties in the decoherence process. Another interesting line of research is the dynamic behavior of the properties under the action of a non-Markovian regime considering the memory effect of the environment.

[1] E. Schrödinger, Naturwissenschaften **14**, 664 (1926).
[2] R. J. Glauber, Phys. Rev. **131**, 2766 (1963).
[3] A. M. Perelomov, Commun. Math. Phys. **26**, 222 (1972).
[4] A. Perelomov, *Generalized Coherent States and Their Applications* (Springer, New York, 1986).
[5] R. Gilmore, Ann. Phys. (N.Y.) **74**, 391 (1972).
[6] J. R. Klauder and B. Skagertam, *Coherent States: Application in Physics and Mathematical Physics* (World Scientific, Singapore, 1985).
[7] S. T. Ali, J.-P. Antoine, and J.-P.Gazeau, *Coherent States, Wavelets and Their Generalizations* (Springer, New York, 2000).
[8] K. Berrada, J. Math. Phys. (N.Y.) **56**, 072104 (2015).
[9] D. Markham and V. Vedral, Phys. Rev. A **67**, 042113 (2003).
[10] C. C. Gerry and A. Benmoussa, Phys. Rev. A **71**, 062319 (2005).
[11] C. C. Gerry and J. Albert, Phys. Rev. A **72**, 043822 (2005).
[12] H. J. Kimble, M. Dagenais, and L. Mandel, Phys. Rev. Lett. **39**, 691 (1977).
[13] R. Short and L. Mandel, Phys. Rev. Lett. **51**, 384 (1983).
[14] R. E. Slusher, L. W. Hollberg, B. Yurke, J. C. Mertz, and J. F. Valley, Phys. Rev. Lett. **55**, 2409 (1985).
[15] B. Yurke and D. Stoler, Phys. Rev. Lett. **57**, 13 (1986).
[16] L. Mandel and E. Wolf, *Optical Coherence and Quantum Optics* (Cambridge University Press, Cambridge, United Kingdom, 1995).
[17] R. L. de Matos Filho and W. Vogel, Phys. Rev. Lett. **76**, 608 (1996).
[18] G. J. Milburn and D. F. Walls, *Quantum Optics* (Springer, New York, 2008).
[19] M. O. Scully, U. W. Rathe, C. Su, and G. S. Agarwal, Opt. Commun. **136**, 39 (1997).
[20] A. Gatti, E. Brambilla, M. Bache, and L. A. Lugiato, Phys. Rev. A **70**, 013802 (2004).
[21] C. H. R. Ooi, B.-G. Kim, and H.-W. Lee, Phys. Rev. A **75**, 063801 (2007).
[22] C. H. R. Ooi, Phys. Rev. A **75**, 043817 (2007).
[23] C. H. R. Ooi, Q. Sun, M. S. Zubairy, and M. O. Scully, Phys. Rev. A **75**, 013820 (2007).
[24] E. A. Sete and H. Eleuch, Phys. Rev. A **89**, 013841 (2014).

[25] E. A. Sete, H. Eleuch, and S. Das, Phys. Rev. A **84**, 053817 (2011).
[26] E. Giacobino, J.-P. Karr, G. Messin, H. Eleuch, and A. Baas, C.R. Phys. **3**, 41 (2002).
[27] E. A. Sete and H. Eleuch, Phys. Rev. A **82**, 043810 (2010).
[28] M. Tsang, Phys. Rev. A **88**, 021801(R) (2013).
[29] T. Yu and J. H. Eberly, Phys. Rev. Lett. **97**, 140403 (2006).
[30] E. Schrödinger, Naturwissenschaften **23**, 807 (1935).
[31] D. F. Walls and G. J. Milburn, Phys. Rev. A **31**, 2403 (1985); G. J. Milburn and D. F. Walls, Phys. Rev. A **38**, 1087 (1988).
[32] S. Mancini and V. I. Man'ko, Europhys. Lett. **54**, 586 (2001).
[33] S. Dey, A. Fring, and L. Gouba, J. Phys. A **45**, 385302 (2012).
[34] A. Fring, L. Gouba, and B. Bagchi, J. Phys. A **43**, 425202 (2010).
[35] A. Kempf, J. Math. Phys. (N.Y.) **35**, 4483 (1994).
[36] M. A. Nielsen and I. L. Chuang, *Quantum Computation and Quantum Information* (Cambridge University Press, Cambridge, United Kingdom, 2000).
[37] H. Fakhri and A. Hashemi, Phys. Rev. A **93**, 013802 (2016).
[38] S. Dey and V. Hussin, Phys. Rev. A **93**, 053824 (2016).
[39] C. Bastos, A. E. Bernardini, O. Bertolami, N. C. Dias, and J. N. Prata, Phys. Rev. D **93**, 104055 (2016).
[40] T. Jurić and A. Samsarov, Phys. Rev. D **93**, 104033 (2016).
[41] S. Dey and V. Hussin, Phys. Rev. D **91**, 124017 (2015).
[42] S. Dey, Phys. Rev. D **91**, 044024 (2015).
[43] V. I. Man'ko, G. Marmo, S. Solimeno, and F. Zaccaria, Int. J. Mod. Phys. A **08**, 3577 (1993).
[44] C. Quesne, J. Phys. A **35**, 9213 (2002).
[45] R. L. de Matos Filho and W. Vogel, Phys. Rev. A **54**, 4560 (1996).
[46] A. Ballesteros, O. Civitarese, and M. Reboiro, Phys. Rev. C **68**, 044307 (2003).
[47] L. C. Biedenharn and M. A. Lohe, *Quantum Group Symmetry and q-Tensor Algebras* (World Scientific, Singapore, 1995).
[48] S. Meljanac, M. Milekovic, and S. Pallua, Phys. Lett. B **328**, 55 (1994).
[49] A. Ballesteros, O. Civitarese, and M. Reboiro, Phys. Rev. C **72**, 014305 (2005).
[50] E. G. Floratos, J. Phys. A **24**, 4739 (1991).
[51] S. S. Avancini and G. Krein, J. Phys. A **28**, 685 (1995).
[52] K. D. Sviratcheva, C. Bahri, A. I. Georgieva, and J. P. Draayer, Phys. Rev. Lett. **93**, 152501 (2004).
[53] S. Ya. Kilin and A. B. Mikhalychev, Phys. Rev. A **85**, 063817 (2012).
[54] S. Mancini and V. I. Man'ko, Euro. Phys. Lett. **54**, 586 (2001).
[55] B. Roy and P. Roy, J. Opt. B **2**, 65 (2000).
[56] V. I. Man'ko, G. Marmo, E. C. G. Sudarshan, and F. Zaccaria, Phys. Scr. **55**, 528 (1997).
[57] S. Dey, A. Fring, and V. Hussin, Int. J. Mod. Phys. B **31**, 1650248 (2017).
[58] T. J. Osborne and M. A. Nielsen, Phys. Rev. A **66**, 032110 (2002).
[59] A. Osterloh, L. Amico, G. Falci, and R. Fazio, Nature (London) **416**, 608 (2002).
[60] A. P. Hines, R. H. McKenzie, and G. J. Milburn, Phys. Rev. A **67**, 013609 (2003).